Ac susceptibility study of a magnetite magnetic fluid

O.E. Ayala-Valenzuela, J.A. Matutes-Aquino, J.T. Elizalde Galindo and C. E. Botez.

Abstract

Magnetite nanometric powder was synthesized from metal salts using a coprecipitation technique. The powders were used to produce magnetic fluid via a peptization method, with hydrocarbon Isopar M as liquid carrier and oleic acid as surfactant. The complex magnetic susceptibility $X=X'+iX''$ was measured as a function of temperature T in steps of 2.5 K from 3 to 298 K for frequencies ranging from f =10 to 10 000 Hz. The magnetic fluid real and imaginary components of the ac susceptibility show a prominent maximum at temperatures that increase with the measuring frequency, which is attributed to a spin-glass-like behavior. The peak temperature T_{p1} of X'' depends on f following the Vogel–Fulcher law $f = f_0 \exp[E/k_B(T_{p1}-T_0)]$, where f_0 and E are positive constants and T_0 is a parameter related to particle interactions. There is another kind of peak temperature, T_{p2}, in the loss factor tan $S=X'' / X'$ which is related to a magnetic aftereffect. The peak temperature T_{p2} is far less than T_{p1} and shows an Arrhenius-type dependence on f.

Introduction

Magnetic fluids are systems with multiple technical applications (in rotating shaft sealing and loudspeakers) and biomedical applications (in hyperthermia and magnetic drug delivery). From the basic and applied viewpoints, it is important to understand the physical behavior of magnetic fluids in the frozen and liquid states.

In this work we describe the fabrication route of a magnetite-based magnetic fluid and discuss its magnetic and structural characterization with emphasis on the temperature and frequency dependence of ac susceptibility in the frozen state. The magnetite nanoparticles were synthesized by coprecipitation. Magnetite is a cubic inverse spinel where the two cations are iron with different valence states. Magnetite have a Verwey transition temperature T_V=120 K where electron hopping ceases and the ferrous ions order in pairs and symmetry is reduced from cubic to triclinic.[1] The magnetitebased magnetic fluid was prepared by a peptization method with Isopar M as liquid carrier and oleic acid as surfactant. The Isopar M–based magnetic fluid freezes at about FP =215 K (the pouring point of Isopar M).

It is well known that if the interaction of the magnetic dipoles of atoms is not strong enough to create a ferromagnetic or antiferromagnetic state but are strong enough compared with the paramagnetic atoms, the material shows a spin-glass state and the complex magnetic susceptibility shows a cusp as a function of temperature and the peak temperature obeys the Vogel–Fulcher law.[2] It was proposed that the peak temperature in the frozen state is connected with the relaxation time according to the Vogel–Fulcher law.[3] On the other hand, if a magnetic material shows a magnetic aftereffect in an ac external magnetic field, the magnetization has a phase lag and the loss factor is expressed by[4,5]

$$\tan \delta = \frac{\zeta \omega \tau_4}{(1+\zeta) + (\omega \tau_4)^2} = \frac{\chi''}{\chi'} .$$

When one plots X’’ / X’ instead of X’’ as a function of temperature, the main peaks of X’’ in the frozen state disappear and one obtains only the peaks corresponding to the shoulders of X’’ as function of T. These new peaks are related to magnetic aftereffects. The physical origin of the aftereffect peaks could be Néel relaxation of nanoparticles or disaccommodation in ferrites. In the former the peak temperatures should change with dilution of nanoparticles in the magnetic fluid, while in the latter they should not change, being a characteristic of colloidal particles. One proposed theory of disaccommodation is electron hopping between Fe^{2+} and Fe^{3+}, and other is related to vacancies in ferrites. Finally, ac susceptibility peaks in melted magnetic fluids may be related to Brown relaxation of the whole nanoparticles.

Experimental

Magnetite nanoparticles were synthesized by chemical coprecipitation from reagent grade chemicals, namely, $FeCl_3\cdot 6H_2O$, $FeCl2\cdot 4H_2O$, and NH_4OH. Stoichiometric ratops (1:2) (Fe^{+2} , Fe^{+3}) at 0.1 *M* solutions were mixed and heated at 343 K with continuous stirring. A black precipitate was obtained after the rapid addition of NH_4OH at 10%. A peptization process at 353 K with continuous stirring at 1000 rpm was used to synthesize the magnetic fluid. For the magnetic fluid the liquid carrier was Isopar M while the surfactant was oleic acid.

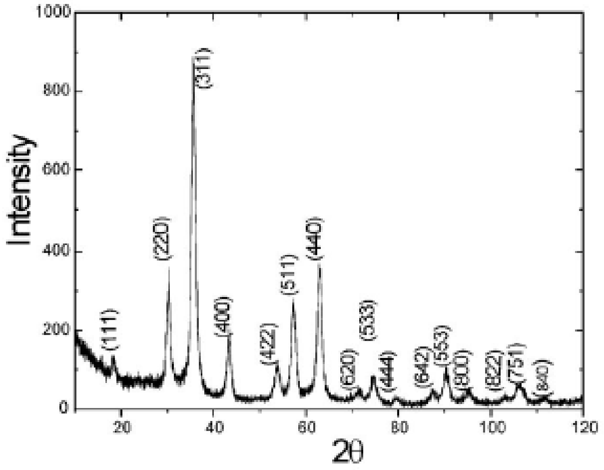

FIG. 1. Cubic spinel magnetite x-ray diffraction pattern.

The magnetization curves of the magnetic nanoparticles and fluid were measured using a VSM LDJ Electronics model 9600 at room temperature. The complex magnetic susceptibility X =X'+X'' of the magnetic fluid was measured as a function of temperature T in steps of 2.5 K from 3 to 298 K for frequencies ranging from f =10 to 10 000 Hz in a Quantum Design physical property measurement system.

Results and discussion

Figure 1 shows the x-ray diffraction pattern of magnetite nanoparticles, showing line broadening typical of nanometric size particles. Figure 2(a) shows the superparamagnetic reversible magnetization curve of the magnetite nanoparticles with a specific magnetization of about 53 emu/g for a applied field of 10 000 Oe. This magnetic field value is insufficient to saturate the powder.

Figure 2(b) shows the superparamagnetic reversible magnetization curve of the magnetic fluid. The specific magnetization is about 5.7 emu/g for an applied field of 10 000 Oe, which is about nine times lower than the corresponding value for the powder, reflecting the dilution degree of the magnetic nanoparticles in the fluid.

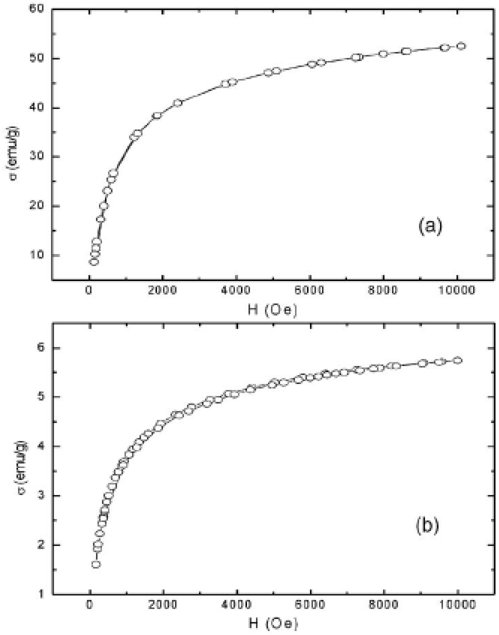

FIG. 2. Reversible magnetization curves of superparamagnetic (a) magnetite nanoparticles and (b) magnetic fluid.

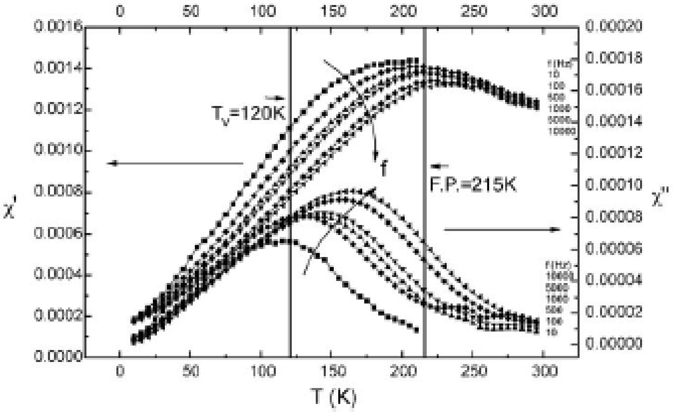

FIG. 3. ac magnetic susceptibility real and imaginary components of magnetic fluid.

Figure 3 shows the real and imaginary components of ac magnetic susceptibility of the magnetite magnetic fluid as a function of temperature for several measuring frequencies. The maxima of the real and imaginary components of susceptibility move to higher temperatures as the measuring frequency increases. The maximum values of the real component decrease as measuring frequency increases because it is more difficult for the particle magnetization to follow the field changes as the applied field frequency increases. On the other hand, the maximum values of the imaginary component of susceptibility increase as measuring frequency increases because the energy losses are greater. The imaginary component of susceptibility shows a shoulder at a temperature lower than the temperature of the maximum. Above the Isopar M pouring point, in the ac susceptibility curves can be observed some small amplitude maxima probably related to Brown relaxation of the whole magnetic nanoparticles when the magnetic fluid is already in the liquid state.

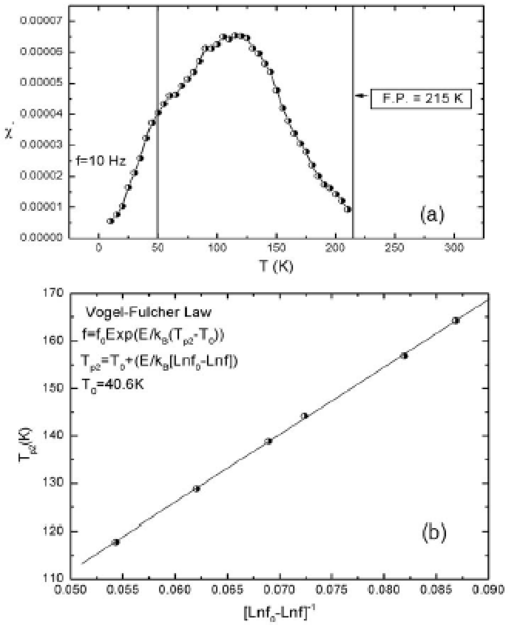

FIG. 4. (a) Magnetic fluid χ'' component as a function of temperature for measuring frequency of 10 Hz. (b) Vogel–Fulcher law fitting for spin-glass-like data with T_0=40.6 K.

Figure 4(a) shows the imaginary component of susceptibility as a function of temperature for a measuring frequency of 10 Hz. It shows a maximum and a shoulder at lower temperature. A similar behavior is observed for other measuring frequencies. We have associated the maxima in X'' with a spin-glass-like behavior following a Vogel–Fulcher law with T_0=40.6 K as shown in Fig. 4(b).[6,7] In the case of an ensemble of superparamagnetic noninteracting uniaxial particles, without an applied magnetic field, the Néel relaxation equation $\mathrm{T} = \mathrm{T}_0 \exp(KV/k_BT)$ with $\mathrm{T}_0 \sim 10^{-9}$ s can be used to determine the relaxation time, where KV is the anisotropy barrier. In the case of an ensemble of interacting particles, an additional interaction energy barrier should be included. This leads to a Vogel–Fulcher law that when expressed in measurement frequency f and peak temperature T_{p1} looks like $f = f_0$ exp□$KV/k_B[T_{p1} - T_0]$), where the parameter T_0 increases with interaction strength. This relation is only valid when $T_0 << T_K$, where $T_K = (KV/k_B)$. In the opposite case of strong coupling a similar expression can be applied again provided that the particle volume V is replaced by a temperature dependent effective volume and the anisotropy constant K is replaced by an effective value to account for the interacting effect.[8–11]

As can be seen from Fig. 5(a), for a measuring frequency of 10 Hz, the shoulder becomes a maximum when we plot the relation X'' /X', instead of X'', as a function of temperature. In this case the peak temperature T_{p2} is 45 K. A similar behavior is found for other measuring frequencies. We have associated the maxima in X'' /X' with a magnetic aftereffect, where the ratio XX'' / X' is equal to the loss factor.4 Figure 5(b) shows an Arrhenius-type law between the period of the measuring frequency and the temperature $T_{p2.}$

Conclusions

The ac susceptibility real and imaginary components of a 10 nm magnetite-based magnetic fluid show maxima that move to higher temperatures as the measuring frequency increases. The real (imaginary) component maximum decreases (increases) as the measuring frequency increases due to magnetization inertia and loss effect. The magnetite frozen magnetic fluid shows spin-glass-like behavior following the Vogel–Fulcher law with an interaction parameter T_0 =40.6 K, and aftereffect peaks that could be fitted with an Arrhenius-type law. The physical origin of the aftereffect peak could be either Néel relaxation of nanoparticles or disaccommodation in ferrite itself. Above the Isopar M pouring point in the ac susceptibility curves there are some small amplitude maxima probably related to Brown relaxation of the whole magnetic nanoparticles already in the liquid state.

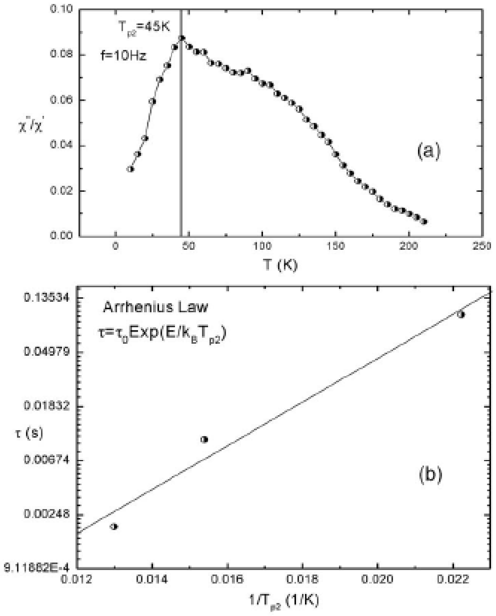

FIG. 5. (a) Magnetic fluid χ''/χ' ratio as a function of temperature for measuring frequency of 10 Hz. (b) Arrhenius law fitting for magnetic after-effect data.

References

1R. Skomski and J. M. D. Coey, Permanent Magnetism (Institute of Physics, Berkshire, 1999).

2K. Binder and A. P. Young, Rev. Mod. Phys. 58, 801 (1986).

3J. Zhang, C. Boyd, and W. Luo, Phys. Rev. Lett. 77, 390 (1996).

4S. Chikazumi, Physics of Magnetism (Kreiger, Huntington, NY, 1978).

5J. I. Gittleman, B. Abeles, and S. Bozowski, Phys. Rev. B 9, 3891 (1974).

6S. Taketomi, Phys. Rev. E 57, 3073 (1998).

7P. C. Morais, J. G. Santos, L. B. Silveira, C. Gansau, N. Buske, W. C. Nunes, and J. P. Sinnecker, J. Magn. Magn. Mater. 272-276, 2328 (2004).

8A. Aharoni, Introduction to the Theory of Ferromagnetism (Clarendon, Oxford, 1996).

9S. Shtrikman and E. P. Wohlfarth, Phys. Lett. 85A, 467 (1981).

10M. Solzi, M. Ghidini, and G. Asti, in Magnetic Nanostructures, edited by H. S. Nalwa (American Scientific, New York, 2002).

11O. Ayala-Valenzuela, J. Matutes-Aquino, R. Betancourt-Galindo, O. Rodríguez-Fernández, P. C. Fannin, and A. T. Giannitsis, J. Appl. Phys. 97, 10Q914 (2005).